On the Performance of Several 2-D Harmonic Retrieval Techniques*

Matthew P. Pepin and Michael P. Clark
Department of Electrical and Computer Engineering
Air Force Institute of Technology
AFIT/ENG, 2950 P. Street, Wright-Patterson AFB, OH 45433-7765

Abstract

This paper investigates the performance of 2-D harmonic retrieval techniques based on two criteria: computational complexity and mean-squared estimation error. Computational complexity is described in terms of order of computation and FLOPS required for an example test case. Mean-square estimation performance is measured for this test case and compared with the Cramér-Rao bound. Each technique is assigned a point in a Cartesian coordinate system with axes corresponding to computation and estimation error.

1 Introduction

The problem of estimating an unknown one-dimensional signal in noise has been heavily researched, especially in the case of damped exponential signals. These techniques can not be simply extended to two-dimensions due to limitations on the polynomial rooting contained in many of these techniques. Recent research, however, has lead to the development of several efficient two-dimensional techniques that exhibit good performance on two-dimensional damped exponential signals in noise. This paper summarizes five of these techniques and measures their performance. The techniques include a state space method developed by Rao and Kung [8], a matrix pencil method by Hua [6], a linear prediction method by Sacchinni, Steedly, and Moses [9], a subspace fitting method by Li, Stoica, and Zheng [7], and a maximum likelihood method by Clark and Scharf [1]. These techniques can be characterized by estimation performance and by computational complexity. Application of any of these techniques to a specific problem involves a trade-off between these. The estimation problem examined in this paper involves a single data instance, for example, a single snapshot from a rectangular sensor array.

*This work is supported by the Advanced Research Projects Agency under grant MDA 972-93-1-0015

1.1 Damped Exponential Models

Many signals can be modeled as the sum of damped exponential signals that vary in two-dimensions:

$$y(m_1, m_2) = \sum_{i=1}^{p}\sum_{j=1}^{q} s_{i,j}\lambda_i^{m_1}\gamma_j^{m_2} + n(m_1, m_2), \quad (1)$$

where $0 \le m_1 \le M_1 - 1$, $0 \le m_2 \le M_2 - 1$, λ_i and γ_j characterize the harmonic in each direction, $s_{i,j}$ is the complex amplitude, and n is complex additive noise. In this paper parameters λ_i, γ_j, and $s_{i,j}$ are assumed deterministic. Equation 1 can be rewritten forming an $M_1 \times M_2$ matrix, Y, with $(m_1, m_2)^{th}$ entry $y(m_1, m_2)$:

$$Y = GSH^T + N, \quad (2)$$

$$G = [\boldsymbol{g}_1 \quad \boldsymbol{g}_2 \quad \dots \quad \boldsymbol{g}_p],\ \boldsymbol{g}_i = \Psi_{M_1}(\lambda_i),$$
$$H = [\boldsymbol{h}_1 \quad \boldsymbol{h}_2 \quad \dots \quad \boldsymbol{h}_p],\ \boldsymbol{h}_j = \Psi_{M_2}(\gamma_j),$$
$$\Psi_d(z) = [1 \quad z \quad z^2 \quad \dots \quad z^{d-1}]^T,$$

and N an is $M_1 \times M_2$ matrix with $(m_1, m_2)^{th}$ entry $n(m_1, m_2)$. G and H contain Vandermonde columns of the harmonics, and S contains the amplitudes.

It is often useful to vectorize (stack the columns of) the matrix representation of the signal:

$$\boldsymbol{y} = (H \otimes G)\boldsymbol{s} + \boldsymbol{n} \quad (3)$$

or

$$\boldsymbol{y} = A\boldsymbol{s} + \boldsymbol{n} \quad (4)$$

where $\otimes$ denotes the Kronecker product, $\boldsymbol{y} = \mathrm{vec}(Y)$, $\boldsymbol{s} = \mathrm{vec}(S)$, and $\boldsymbol{n} = \mathrm{vec}(N)$.

Notice that equation 1 forces the 2-D harmonics to lie on a grid. If we generalize the model by removing this restriction then we force S to be diagonal. Eliminating the rows in equation 3 where $s_k = 0$ gives

$$A = [\boldsymbol{h}_1 \otimes \boldsymbol{g}_1 \quad \boldsymbol{h}_2 \otimes \boldsymbol{g}_2 \quad \dots \quad \boldsymbol{h}_p \otimes \boldsymbol{g}_p] \quad (5)$$

and $\boldsymbol{s}$ now contains just the diagonal elements of S.

For this analysis, circular white Gaussian noise is used such that $\mathrm{E}(\boldsymbol{n}^*\boldsymbol{n}) = \sigma^2 I$ and $E(\boldsymbol{n}^T\boldsymbol{n}) = 0$, where $(\cdot)^*$ denotes complex conjugate transpose.

1.2 A Least Squares Formulation

For a single data instance the maximum likelihood estimate of the parameters of equation 2 is given by the solution to the optimization problem

$$\min_{\lambda_i,\gamma_j,s_k} \|Y - GSH^T\|_F, \tag{6}$$

or in terms of equation 3

$$\min_{\lambda_i,\gamma_j,s_k} \|\boldsymbol{y} - A\boldsymbol{s}\|_2. \tag{7}$$

Given λ_i and γ_j, A can be constructed, and $\boldsymbol{s}$ is the least squares solution of equation 7, $\boldsymbol{s} = (A^*A)^{-1}A^*\boldsymbol{y}$. Substituting this into equation 7 gives

$$\min_{\lambda_i,\gamma_j} \|(I - A(A^*A)^{-1}A^*)\boldsymbol{y}\|_2^2 = \min_{\lambda_i,\gamma_j} \mathrm{tr}(\boldsymbol{P}_A^{\perp}\, \boldsymbol{y}\boldsymbol{y}^*), \tag{8}$$

where $\boldsymbol{P}_A^{\perp}$ is the projection onto the subspace orthogonal to the signal subspace (the range of A) defined by parameters, λ_i and γ_j: $\boldsymbol{P}_A^{\perp} = I - A(A^*A)^{-1}A^*$.

In several methods the minimization problem is reformulated in terms of the projections onto the subspaces orthogonal to the ranges of G and H. [1, 7]. Specifically, the projection, $\boldsymbol{P}_G^{\perp}$, can be written in terms of an annihilation matrix C whose range is the subspace orthogonal to the signal subspace: $C^*G = 0$. Then $\boldsymbol{P}_G^{\perp} \equiv C(C^*C)^{-1}C^*$ with

$$C^* \equiv C_p^* \equiv \begin{bmatrix} c_p & \cdots & c_1 & c_0 & 0 \\ & \ddots & \ddots & \ddots & \\ 0 & c_p & \cdots & c_1 & c_0 \end{bmatrix}. \tag{9}$$

Here the $(M_1-p)\times M_1$ matrix C^* contains coefficients, $\{c_i\}_{i=0}^{p}$, of a polynomial that annihilates the λ_i. The two one-dimensional optimizations are then

$$\min_{\lambda_i} \boldsymbol{y}^*(I \otimes \boldsymbol{P}_G^{\perp})\boldsymbol{y}, \tag{10}$$

$$\min_{\gamma_j} \boldsymbol{y}^*(\boldsymbol{P}_H^{\perp} \otimes I)\boldsymbol{y}, \tag{11}$$

where $\boldsymbol{P}_H^{\perp} \equiv D(D^*D)^{-1}D^*$ such that $D^*H = 0$.

The 1-D problem may also be formulated as

$$\min_{\gamma_j} \boldsymbol{d}^*\tilde{Y}^*((D^*D)^{-1} \otimes I)\tilde{Y}\boldsymbol{d}, \tag{12}$$

with $\boldsymbol{d} = [d_p \quad d_{p-1} \quad \cdots \quad d_0]$ by arranging the length M_1M_2 vector $\boldsymbol{y}$ in a $M_1(M_2-p) \times (p+1)$ matrix,

$$\tilde{Y} \equiv [\tilde{Y}_{p+1}(0) \quad \tilde{Y}_{p+1}(1) \quad \cdots \quad \tilde{Y}_{p+1}(M_1-1)]^T \tag{13}$$

$$\tilde{Y}_p(k) = \begin{bmatrix} y(k,0) & y(k,1) & \cdot & y(k,M_2-p) \\ y(k,1) & y(k,2) & \cdot & y(k,M_2-p+1) \\ \vdots & \vdots & \cdot & \vdots \\ y(k,p-1) & y(k,p) & \cdot & y(k,M_2-1) \end{bmatrix} \tag{14}$$

where $\tilde{Y}\boldsymbol{d} = (D^* \otimes I)\boldsymbol{y}$ with $C = D$ in equation 9.

In another approach an approximate solution to equation 6 is obtained in one dimension by exploiting rotational invariance between subarrays of the principal components of Y [6, 8]. First, the principal components of Y are obtained through the singular value decomposition (SVD) of Y : $Y = U\Sigma V^*$. The principal components of Y are the columns of U and V corresponding to the p largest singular values in Σ. These combine to give a rank-p approximation of Y,

$$Y_s = U(:,1:p)\Sigma(1:p,1:p)V(:,1:p)^* \equiv U_s\Sigma_s V_s^*. \tag{15}$$

Subarrays of Y_s can be formed by separately removing the last and first row of G giving $G_0 = G(1:N-1,:)$ and $G_1 = G(2:N,:)$. These are related by

$$G_1 = G_0F_G \tag{16}$$

with $F_G = \mathrm{diag}([\lambda_1 \quad \lambda_2 \quad \cdot \quad \lambda_p])$. Since U_s forms a basis for the range of G there is an invertible T_G where

$$\begin{bmatrix} G_0 \\ G_0F_G \end{bmatrix} = \begin{bmatrix} U_0 \\ U_1 \end{bmatrix} T_G. \tag{17}$$

Here $U_0 = U_s(1:N-1,:)$ and $U_1 = U_s(2:N,:)$. Premultiplying both sides by $(G_0)^+$ gives

$$\begin{bmatrix} I \\ F_G \end{bmatrix} = \begin{bmatrix} G_0^+U_0 \\ G_0^+U_1 \end{bmatrix} T_G. \tag{18}$$

where $(\cdot)^+$ denotes pseudoinverse. Solving the first equation of 18 for G_0^+; substituting in the second gives

$$F_G = T_G^{-1}U_0^+U_1T_G, \tag{19}$$

for a matrix T_G. The λ_i are thus eigenvalues of $U_0^+U_1$.

2 Two-Dimensional Techniques

2.1 State Space

The state space technique [8] performs the minimization of equation 6 through a low rank approximation to Y. The harmonics are obtained by splitting

the principal components SVD in equation 15 to separately attain F_G and F_H.

Now, Y_s can be expressed as

$$Y_s = U_s \Sigma_s V_s^* = G S H^T. \tag{20}$$

The ranges of U_s and G and the null spaces of V_s^* and H^T must be the same. Thus there exist nonsingular matrices T_G and T_H such that $G = U_s T_G$ and $H^T = T_H^T V_s^*$. G and H can be segmented as in equation 16. Equation 19 then gives $F_G = T_G^{-1} U_0^+ U_1 T_G$ and $F_H = T_H^{-1} \text{conj}(V_0^+ V_1) T_H$.

From 20 the least squares solution for S is

$$S = G^+ Y_s (H^T)^+ = T_G^{-1} \Sigma_s T_H^{-T}. \tag{21}$$

Eigenvalues of F_G and F_H, λ_i and γ_j, are paired by (i,j) location of the maximum of each column of S. The matching in [8] uses a similar estimate of S.

The SVD of and $k \times l$ matrix is $O(kl^2 + l^3)$ [4]. Computation of the SVD of the Y in equation 20 requires the majority of computations for this technique making it an $O(N^3)$ technique where $N = M_1 = M_2$.

2.2 MEMP

The MEMP technique [6] performs the minimization of equation 6. The data matrix Y is replaced with a block Hankel matrix $\tilde{Y}$ with the same range (size parameters have been set equal to p for this paper):

$$\tilde{Y} = \begin{bmatrix} \tilde{Y}_p(0) & \tilde{Y}_p(1) & \cdots & \tilde{Y}_p(M_1-p) \\ \tilde{Y}_p(1) & \tilde{Y}_p(2) & \cdots & \tilde{Y}_p(M_1-p+1) \\ \vdots & \vdots & \ddots & \vdots \\ \tilde{Y}_p(p-1) & \tilde{Y}_p(p) & \cdots & \tilde{Y}_p(M_1-1) \end{bmatrix} \tag{22}$$

where $\tilde{Y}_p(k)$ is defined in equation 14. Using equation 16 with the last and first p rows in $\tilde{Y}$ removed the principal components of $\tilde{Y}$ and equation 19 give the λ_i. Next, rows of $\tilde{Y}$ are switched for columns with

$$P = [\, \boldsymbol{e}_1 \quad \boldsymbol{e}_{1+2p} \quad \cdot \quad \boldsymbol{e}_{1+(p-1)p} \quad \cdots \quad \boldsymbol{e}_{p+(p-1)p} \,]^T,$$

where $\boldsymbol{e}_i$ is the i_{th} component of the natural basis. The principal components of $P\tilde{Y}$ then give the γ_j.

The harmonics can be matched by successively finding the distinct pairs (λ_i, γ_j) that maximize

$$\sum_{t=1}^{p} \| \boldsymbol{u}_t^* \, (\boldsymbol{g}_i \otimes \boldsymbol{h}_j) \|^2 \tag{23}$$

where $U_s = [\, \boldsymbol{u}_1 \quad \boldsymbol{u}_2 \quad \ldots \quad \boldsymbol{u}_p \,]$ contains the p principal eigenvectors of $\tilde{Y}$. For distinct harmonics the matching method of equation 21, however, is more accurate. S is estimated by forming G and H and calculating the least squares solution $S = G^+ Y (H^T)^+$.

Computation of the first l columns of U in the SVD of an $k \times l$ matrix is $O(kl^2)$ [4]. Computation of U_s, or V_s in the SVD of the $(M_1-p+1)(M_2-p+1) \times p^2$ matrix $\tilde{Y}^*$, dominates making this an $O(p^4 N^2)$ technique where $N = M_1 = M_2$ and $p \ll N$.

2.3 2-D Prony

The 2-D Prony technique [9] estimates a solution to the equation error formulation of equation 12: $\tilde{Y}\boldsymbol{d} = \boldsymbol{e}$. Estimation is done twice in each dimension. In the estimation the expected number of harmonics p and q is overfit with $p^+ \geq p$ and $q^+ \geq q$. After estimation, only the p harmonics λ_i and the q harmonics γ_j with the highest energy are retained. For this paper $p^+ \equiv q^+ \equiv \frac{3}{4} M_1 \equiv \frac{3}{4} M_2$. First, $\tilde{Y}$ is found from

$$\tilde{Y}\boldsymbol{d} = (D_{q^+}^* \otimes I)\boldsymbol{y}_r \tag{24}$$

as in equation 13 with $\boldsymbol{y}_r = \text{vec}(Y^T)$. $\boldsymbol{d}$ is estimated by

$$\boldsymbol{d} = [\, (V_2 V_1^* / \|V_1\|^2) \quad 1 \,]^T, \tag{25}$$

where $V_2 = V_s(2{:}\text{length}(V), p+1{:}p^+)$, $V_1 = V_s(1, p+1{:}p^+)$, and V_s are the right p principal singular vectors of $\tilde{Y}$. The roots of $\boldsymbol{d}$ are the first estimate of the γ_j and are defined as $\boldsymbol{\gamma}_1$. Solving for $S = Y(H^T)^+$ each column of S, $\boldsymbol{s}_k$, can then be used to find the λ_i giving estimates defined as $\boldsymbol{\lambda}_i$ for each element of $\boldsymbol{\gamma}_1$. Construct $\tilde{S}$ from

$$\tilde{S}_{p^+ +1}\boldsymbol{d} = D_{p^+}^* \boldsymbol{s}_k \tag{26}$$

as in equation 14. The roots of $\boldsymbol{d}$ give $\boldsymbol{\lambda}_i$. This procedure is repeated on $\boldsymbol{y}_c = \text{vec}(Y)$ and the rows of $S = G^+ Y$ to obtain $\boldsymbol{\lambda}_2$ and their $\boldsymbol{\gamma}_j$. The $\lambda_i = [\boldsymbol{\lambda}_1]_i$ and $\gamma_j = [\boldsymbol{\gamma}_2]_j$ are matched by successively pairing the harmonics with closest second estimates in $\boldsymbol{\lambda}_i$ and $\boldsymbol{\gamma}_j$.

The SVD of the $M_1(M_2 - \frac{3}{4}M_2) \times \frac{3}{4}M_2 + 1$ matrix $\tilde{Y}$ in equation 24 dominates the computation making this an $O(N^4)$ technique where $N = M_1 = M_2$.

2.4 2-D Mode

The 2-D MODE technique [7] minimizes equation 8. In terms of $\boldsymbol{P}_G^\perp$ and $\boldsymbol{P}_H^\perp$ equation 8 is

$$\min_{\lambda_i, \gamma_j} \text{tr}((\boldsymbol{P}_H^\perp \otimes I + I \otimes \boldsymbol{P}_G^\perp - \boldsymbol{P}_H^\perp \otimes \boldsymbol{P}_G^\perp)\, \boldsymbol{y}\boldsymbol{y}^*), \tag{27}$$

where the last Kronecker product is high order and neglected. With $Z = \boldsymbol{y}\boldsymbol{y}^*$ the minimization for λ_i is

$$\min_{\lambda_i} \text{tr}(I \otimes \boldsymbol{P}_G^\perp) Z = \min_{\lambda_i} \text{tr} \boldsymbol{P}_G^\perp Z_\lambda \tag{28}$$

where $Z_\lambda \equiv \sum_{m_1=0}^{M_1-1} Z_{m_1 m_1}$ and $Z_{ij} = Z(iM_2+1 : (i+1)M_2, jM_2+1 : (j+1)M_2)$ is an $M_2 \times M_2$ submatrix of Z. The minimization for γ_i is

$$\min_{\gamma_j} \mathrm{tr}(\boldsymbol{P}_H^{\perp} \otimes I) Z = \min_{\gamma_j} \mathrm{tr} \boldsymbol{P}_H^{\perp} Z_\gamma$$

where $(Z_\gamma)_{ij} \equiv \mathrm{tr}(Z_{ij})$. Using C from equation 9 the minimizations are done with MODE iterations

$$\min_{\boldsymbol{c}_{n+1}} \boldsymbol{c}_{n+1}^* \tilde{Y}^* (C^* C)_n^{-1} \tilde{Y} \boldsymbol{c}_{n+1}, \tag{29}$$

where $\tilde{Y} = [\tilde{U}_1 \quad \tilde{U}_2 \quad \ldots \quad \tilde{U}_p]^T$ is defined such that

$$\tilde{U}_i^T \boldsymbol{c} = C^* \boldsymbol{u}_i. \tag{30}$$

Here $U_\lambda = [\boldsymbol{u}_1 \quad \boldsymbol{u}_2 \quad \ldots \quad \boldsymbol{u}_p]$ contains the p principal eigenvectors of Z_λ. The band diagonal Cholesky decomposition of the kernel $(C^* C)^{-1}$ greatly speeds computations [5]. The minimizing $\boldsymbol{d}$ from equation 11 is similarly attained. The harmonics, λ_i and γ_j, are then the roots of the polynomials given by $\boldsymbol{c}$ and $\boldsymbol{d}$. Matching is done with the method of equation 21.

Computation of the SVD of Z_λ and Z_γ dominates making this an $O(N^3)$ technique where $N = M_1 = M_2$.

2.5 2-D IQML

The 2-D IQML technique [1] performs the minimization in equation 10 using the model in equation 5. In the case of circular white Gaussian noise

$$\boldsymbol{P}_A^{\perp} \equiv W (W^* W)^+ W^*, \tag{31}$$

where $(\cdot)^+$ denotes pseudoinverse and

$$W^* = \begin{bmatrix} I_{M_2} \otimes C_p^* \\ [I_{M_2-1} | 0] \otimes D_{p-1}^* - [0 | I_{M_2-1}] \otimes \hat{I} \end{bmatrix} \tag{32}$$

where $\hat{I} = [I_{M_1-p+1} \quad 0_1 \quad \ldots \quad 0_{p-1}]$ and C_p^* and D_{p-1}^* are defined as in equation 9. The upper block of W^* annihilates the harmonics in one direction, λ_i and the lower block of W^* predicts the harmonics in the second dimension, γ_j based on the harmonics annihilated in the first dimension. The minimization is performed with IQML-like iterations,

$$\min_{\boldsymbol{f}_{n+1}} \boldsymbol{f}_{n+1}^* \tilde{Y}^* (W^* W)_n^+ \tilde{Y} \boldsymbol{f}_{n+1}, \tag{33}$$

where $\boldsymbol{f} = [\boldsymbol{c} \quad \boldsymbol{d}]^T$ and $\tilde{Y}$ is defined such that

$$\tilde{Y} \boldsymbol{f} = W^* \boldsymbol{y}. \tag{34}$$

Computations can be reduced from $O(N^6)$ ($N = M_1 = M_2$; $p \ll N$) for the SVD in $(W^* W)^+$ when this is replaced with the normal inverse by using a permutation matrix P to choose $M_1 M_2 - p$ linearly independent rows of the banded matrix W^* [3]. With the $(M_1 M_2 - p) \times (M_1 M_2 - p)$ matrix $P W^* W P^*$ 33 is

$$\min_{\boldsymbol{f}_{n+1}} \boldsymbol{f}_{n+1}^* \tilde{Y}^* P^* (P W^* W P^*)_n^{-1} P \tilde{Y} \boldsymbol{f}_{n+1}. \tag{35}$$

Each of the Kronecker products in W^* is a upper band matrix with the last having the largest bankwidth N. Thus there exists a matrix PW^* with bandwidth N and a band Cholesky solution to 35 is $O(N^4)$ [4].

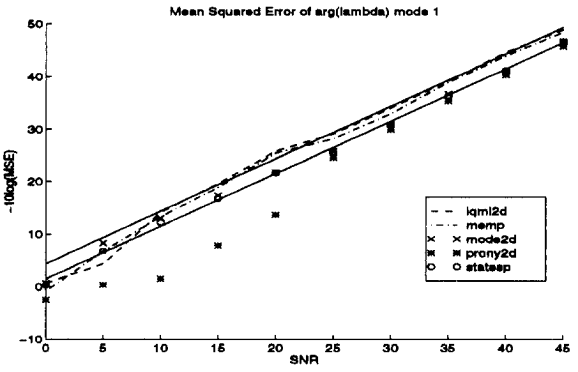

Figure 1: Estimation Accuracy in First Dimension

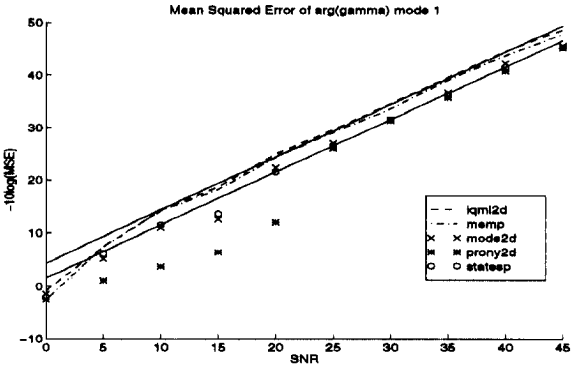

Figure 2: Estimation Accuracy in Second Dimension

3 Results

To illustrate the performance of these techniques a simple example was chosen where two harmonics and white Gaussian noise are present in a 4×4 snapshot. The test case involves harmonics with $(s, \lambda, \gamma) = \{(0.9e^{-j0.1\pi}, 0.97e^{-j0.2\pi}, e^{j0.2\pi}), (e^{j0.2\pi}, 1, 0.95e^{j0.4\pi})\}$. These harmonics are within one Fourier resolution bin.

3.1 Algorithm Performance

Mean Square Error's (MSE's) were calculated using Monte Carlo simulations each with 100 independent experiments at several SNR's ranging over 0-45 dB in

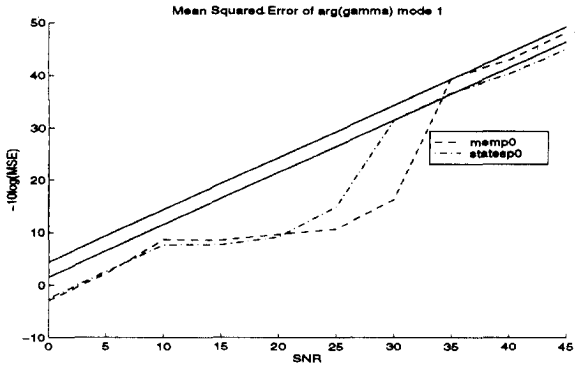

Figure 3: Estimation Accuracy w/ Original Matching

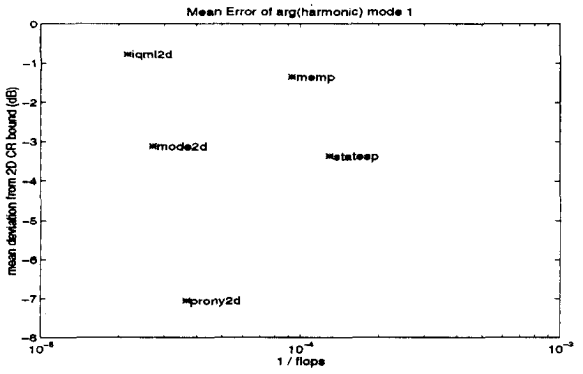

Figure 4: Algorithm Performance (Best Matching)

5 dB increments where SNR $= \frac{\mathrm{tr}(s^* A^* A s)}{M_1 M_2 \sigma^2}$. The results are displayed with the Cramér-Rao(CR) bound for both the two dimensional model and a multiple trial one dimensional model [2]. Figures 1 and 2 show the CR bounds and resultant MSE's for estimated angles for both dimensions. Two solid lines are displayed; the upper is the 2-D CR bound and the lower the multitrial 1-D bound. Figure 3 shows performance with original matching methods. Due to the fact that we sort the first dimension angles in order to compare with the true angles matching errors are manifested solely in the second dimension.

Each technique was coded in MATLAB and the FLOPS for these implementations were computed. Reciprocal FLOPS for each technique are plotted in Figure 4 against the mean deviation of the harmonic angle from the 2-D CR bound. The deviation is computed by averaging the deviation in dB over the angles of both dimensions and all SNRs.

In harmonic angle estimation 2-D IQML and MEMP asymptotically approach the 2-D CR bound. The remaining techniques approach the 1-D CR bound. For overall estimation performance and computation MEMP and state space are the most efficient.

3.2 Conclusions

All techniques perform quite close to the appropriate CR bound. In this specific test case, for harmonic estimation with one data instance 2-D IQML, and MEMP are true two-dimensional techniques and attain the 2-D CR bound. These results are drawn from a single test case. Their applicability to a broad set of array sizes, number of harmonics, and parameter characteristics is still under investigation. Further optimization of the algorithms is also possible. The computational performance of state space, and MODE may be improved with the fast subspace decomposition in [10] which optimizes the $O(N^3)$ rank-p SVD to $O(N^2 p)$.

References

[1] Clark, M. P., and L. L. Scharf, "Two-Dimensional Modal Analysis Based on Maximum Likelihood," IEEE Trans SP 42:6, pp. 1443-1461, June 1994.

[2] Clark, M. P., "Cramér-Rao Bounds for Two-Dimensional Deterministic Modal Analysis," Proc. 27th Asilomar Conf. on Signals, Systems, and Computers, October 1993.

[3] Clark, M. P., and L. L. Scharf, "A Maximum Likelihood Estimation Technique for Spatial-Temporal Modal Analysis," Proc. 25th Asilomar Conf. on Signals, Systems, and Computers, October 1991.

[4] Golub, G. H., and C. F. Van Loan, *Matrix Computations.* Johns Hopkins Univ. Press, Baltimore, 1989.

[5] Hua, Y., "The Most Efficient Implementation of the IQML Technique," IEEE Trans SP 42:8, p. 2203-2204, August 1994.

[6] Hua, Y., "Estimation Two-Dimensional Frequencies by Matrix Enhancement and Matrix Pencil," IEEE Trans SP 40:9, pp. 2267-2280 September 1992.

[7] Li, J., P. Stoica, and D. Zheng, "An Efficient Algorithm for Two-Dimensional Frequency Estimation," (awaiting publication).

[8] Bhaskar Rao, D. V., and S. Y. Kung, "A State-Space Approach for the 2-D Harmonic Retrieval Problem," Proc. Int. Conf. Acoustics, Speech, and Signal Processing, pg. 4.10.1-4.10.4, April 1994.

[9] Sacchinni, J. J., W. M. Steedly, and R. L. Moses, "Two-Dimensional Prony Modeling and Parameter Estimation," IEEE Trans SP 41:11, p. 3127, November 1993.

[10] Xu, G., and T. Kailath, "Fast Subspace Decomposition," IEEE Trans SP 42:3, pp. 539-538, March 1994.